Soft Matter

Cite this: *Soft Matter*, 2011, **7**, 10620

www.rsc.org/softmatter

PAPER

Effect of copolymer compatibilizer sequence on the dynamics of phase separation of immiscible binary homopolymer blends

Ravish Malik, Carol K. Hall* and Jan Genzer

Received 8th July 2011, Accepted 23rd August 2011
DOI: 10.1039/c1sm06292a

We present the results of kinetic Monte Carlo simulations aimed at exploring the effect of copolymer sequence distribution on the dynamics of phase separation of an immiscible A/B binary homopolymer blend. Diblock, protein-like copolymers (PLCs), simple linear gradient, random, and alternating copolymers having equal number of A and B segments, identical chemical composition, and chain length are considered as compatibilizers. All copolymers, irrespective of their sequence, retard the phase separation process by migrating to the biphasic interface between the A/B interface, thereby minimizing the interfacial energy and promoting adhesion between the homopolymer-rich phases. As expected, diblock copolymers perform the best and each block of the diblock copolymer penetrates the energetically favorable homopolymer-rich phase. Alternating copolymers lie at the interface and PLCs, simple linear gradient, and random copolymers weave back and forth across the interface. The weaving and penetration is more pronounced for PLCs than for simple linear gradient and random copolymers. Judging by the contact analysis, extension and conformation of the copolymers at the interface, and structure factor calculations, it is evident that for the chain lengths considered in our simulations, PLCs are better compatibilizers than alternating and random copolymers, while being on a par with simple linear gradient copolymers, but not as good as diblocks.

Introduction

Polymer blends represent an effective route to formulating novel soft materials because their properties can be tuned by varying the composition and types of polymers that are mixed. Polymer blending is, however, challenging because the constituent polymers are often immiscible; the entropic gain upon mixing cannot compensate for the enthalpic losses due to unfavorable interactions. As a consequence most polymer blends tend to macro-phase separate, thereby limiting their utility. Compatibilizers are typically added to overcome these difficulties. They segregate preferentially at the interface between the immiscible homopolymers, reducing interfacial tension and increasing structural integrity and homogeneity, thereby leading to improved stability and mechanical strength of the interface.

In this study we investigate the effects of copolymer compatibilizer sequence on the dynamics of phase separation in immiscible binary homopolymer blends. While diblock copolymers have come to be viewed as the compatibilizer of choice, their tendency to microphase separate at higher copolymer loading[1–5] has led to utilization of other copolymer sequences as compatibilizers.[6–21] Here we consider diblock, protein-like, simple linear gradient random, and alternating copolymers with particular focus on the relative merits of the first three. Gradient copolymers[12–21] have been proposed as an alternative to diblock copolymers as compatibilizers because they do not microphase separate easily at higher copolymer loading. Protein-like copolymers (PLCs) might also serve effectively as compatibilizers as was suggested by our recent computer simulations studies of the equilibrium properties of PLCs, diblock, random, and alternating copolymer compatibilizers.[22] More recently we explored the dynamics of phase separation in an immiscible binary blend compatibilized by PLCs[23] and found that PLCs succeeded in slowing down the process of phase separation.

Protein-like copolymers (PLCs) represent a new class of functional copolymers that exhibit large-scale compositional heterogeneities and long-range correlations along the co-monomer sequence.[24–26] The concept of PLCs was first introduced by Khokhlov and coworkers[24,25] who employed computer simulations to demonstrate that random copolymers with tunable monomer sequences could be generated by adjusting the compactness of a parent homopolymer composed of monomers A, and then converting those segments exposed to the outer periphery of the collapsed coil into B units by reacting the original A monomers with other chemical species present in the surrounding solution. Gradient copolymers are novel copolymers whose composition changes gradually along the chain from one species to the other. They are synthesized routinely *via*

Department of Chemical & Biomolecular Engineering, North Carolina State University, Raleigh, North Carolina, 27695-7905, USA

several polymerization methods, most frequently by controlled free radical polymerization.[14,27–32]

The co-monomer sequence along the copolymer compatibilizer is expected to play an important role in governing the phase behavior and interfacial characteristics of the immiscible polymer blend to be compatibilized. This was demonstrated by Ko *et al.*[7] who used lattice MC simulations to explore the effect of compatibilizer sequence distribution on the phase separation dynamics of immiscible binary blends. They considered diblock, alternating, random, random-alternating, and random-block copolymer sequences as compatibilizers. Their simulation results suggested that diblock copolymers were best at retarding the phase separation followed by random-block, random, random-alternating, and alternating copolymers. Ko *et al.*[7] did not consider PLCs and gradient copolymer sequences.

In this work, we use kinetic Monte Carlo simulation based on the bond fluctuation model (BFM)[33] to investigate the effects of the copolymer compatibilizer sequence on the phase separation dynamics of an immiscible binary blend of homopolymers to which diblock, random, alternating, PLCs, and simple linear gradient copolymer are added.

The binary system contains 9736 20-mers of homopolymer A and 2434 20-mers of homopolymer B. The blends are compatibilized by adding 180 70-mer copolymers containing equal numbers of A and B monomers in the copolymer. Diblock, protein-like, simple linear gradient, random, and alternating copolymers made of A and B units are considered as copolymer compatibilizers. Both the binary blend (A/B) and ternary blend (A/B/A-*co*-B) are mixed uniformly in the initial state. Phase separation between homopolymers A and B is induced by introducing positive pairwise interaction energies between monomer A and B units. As the immiscible polymer blend phase separates, homopolymer A-rich and homopolymer B-rich domains start to form and grow with time. This process is retarded in the compatibilized blend as the copolymers localize to the biphasic A/B interface between the two homopolymers, minimizing the unfavorable interactions and interfacial tension.

To establish the efficacy of the various copolymer sequences and monitor the process of phase separation, the normalized numbers of contacts between segments A–A ($\langle n_{AA}(t)\rangle/\langle n_{AA}(0)\rangle$), B–B ($\langle n_{BB}(t)\rangle/\langle n_{BB}(0)\rangle$), and A–B ($\langle n_{AB}(t)\rangle/\langle n_{AB}(0)\rangle$) are recorded where $t = 0$ refers to the initial homogenous state and t refers to time elapsed after the phase separation commences. The extent of penetration of copolymers into the homopolymer-rich phase over time is monitored by recording the fraction of contacts made by the copolymer segments, A′ and B′, with the two different homopolymer segments A and B, $f_{A'A}(t)$, $f_{A'B}(t)$, $f_{B'A}(t)$, and $f_{B'B}(t)$. The degree of copolymer chain expansion with time is monitored by evaluating the normalized radius of gyration $\langle R_g^2(t)\rangle/\langle R_g^2(0)\rangle$ of the copolymer. The dynamics of phase separation in both the binary and the ternary blend is monitored using the time dependent collective structure factor, $S(q, t)$. The conformation of the different copolymers at the interface is evaluated in order to investigate the mechanism by which the copolymers stabilize the interface.

Highlights of our results are as follows. In the ternary compatibilized blend all copolymers irrespective of their sequence localize to the biphasic interface between the two immiscible homopolymers, minimizing the unfavorable enthalpic interactions and interfacial tension, thereby retarding the process of phase separation. Diblock copolymers are the most effective compatibilizers followed by PLCs and simple linear gradient (which have similar effectiveness), random, and alternating copolymers. This ranking is based on ranking their performance according to the following criteria: an ideal compatibilizer should maximize the normalized number of contacts between A–B segments, minimize the normalized number of contacts between B–B segments, stretch the most at the interface and maximize the number of energetically favorable contacts between the copolymer-homopolymer segments A′–A and B′–B. In addition, based on the structure factor $S(q, t)$ calculations, diblock copolymers slow down the phase separation most effectively followed by PLCs and simple linear gradient copolymers (which perform similarly), random, and alternating copolymers. The conformation of the copolymers at the interface differs from type to type with diblock copolymers penetrating the energetically-favorable homopolymer-rich phase, the alternating copolymers laying at the interface, and the PLCs, simple linear gradient and random copolymers weaving back and forth across the interface. The weaving is more pronounced for PLCs than for the random copolymers but similar to that of simple linear gradient copolymers.

In the next section, we describe the MC method and the generation of simple linear gradient copolymers and PLCs *via* the instant coloring procedure of Khokhlov and co-workers. The following section presents the simulation results for various copolymer sequences. The final section concludes with a short summary of the results and a discussion.

Model and method

The A/B binary blend system consists of 9736 20-mers of type A and 2434 20-mers of type B. The ternary (compatibilized) blend contains the binary blend plus 180 70-mer copolymer chains ($\approx$4.92% of total number of segments in the ternary blend system) each of which consists of monomers of types A and B with composition $x_A = x_B = 0.5$, where x_i is the mole fraction of component i. The copolymer sequences considered include: diblock (A-*b*-B), PLC (A-*plc*-B), simple linear gradient (A-*slg*-B), random (A-*ran*-B), and alternating (A-*alt*-B). The polymers are modeled as self-avoiding walks on a three-dimensional cubic lattice. The phase separation of homopolymer chains A and B is induced by introducing positive repulsive pairwise interaction energy between A and B units $\varepsilon_{AB} = \varepsilon_{AB}'/k_BT = 0.5$, where k_B is the Boltzmann constant and T is the absolute temperature, in both the binary and ternary blend systems. The interaction energies between identical segments are set to zero ($\varepsilon_{AA} = \varepsilon_{BB} = 0$). Additionally the interaction energies between each segment type and the empty sites on the lattice are set to zero. To calculate the energy of the system we need to decide on a range of the interactions; this is usually reported in terms of the number of nearest neighbors to any site that experience an interaction. The MZCCL (the eighteen vectors obtained by all the sign inversions and permutation of the two vector families $P(1, 0, 0) \cup P(1, 1, 0)$ between segments assuming one of the segments is located at (0, 0, 0)) interaction range was chosen.

The lattice Monte Carlo (MC) simulations are based on the three-dimensional bond fluctuation model (BFM)[33] and are performed in the NVT canonical ensemble. We chose the BFM

to model the dynamics of phase separation in polymer blends since it has been utilized previously[34–37] to predict the properties of dense polymer melts. In the BFM each monomer represents a Kuhn segment and occupies eight sites on a simple cubic lattice. Successive monomers along the chain are connected *via* a predetermined set of bond vectors. In order to avoid bond crossing and monomer overlap, the bond vectors are derived from all possible permutations and sign inversions of the following six vector families: $P(2, 0, 0) \cup P(2, 1, 0) \cup P(2, 1, 1) \cup P(2, 2, 1) \cup P(3, 0, 0) \cup P(3, 1, 0)$. For example, all possible permutations and sign inversions of the vector family $P(2, 0, 0)$ yield the following six distinct bond vectors: (2,0,0), (−2,0,0), (0,2,0), (0,−2,0), (0,0,2), and (0,0,−2). Repeating this process for all of the six vector families leads to a total of 108 bond vectors and 87 bond angles. Thus, the model possesses some of the flexibility associated with an off-lattice model while maintaining the advantages associated with working on a lattice, such as integer arithmetic and parallelization.[38] The MC algorithm is executed in the following manner. First a monomer unit is chosen at random and translated by one lattice spacing in a direction chosen randomly out of the six possible directions. Next a check is made to verify that the resulting move does not violate the excluded volume and bond constraints set forth by the BFM. If it does, the move is rejected and the monomer is restored to its original position. If all of the BFM constraints are satisfied, the Metropolis sampling rule is applied, *i.e.*, the move is accepted with a probability equal to $min(1, \exp(-\Delta E/k_BT))$, where ΔE is the energy change due to the move. The MC simulations are performed on a simple cubic lattice of $L \times L \times L$ sites with $L = 80$. The volume fraction, $\phi = N/L^3$, for the pure as well as compatibilized blend is set to $\phi = 0.5$, where N is the number of beads in the simulation box. Periodic boundary conditions are imposed in all three directions (x, y, and z) to overcome the limitation of finite system size.

We now justify our choice of 20-mers homopolymers and 70-mer copolymers used in our simulations. Ideally we want the homopolymers to be much longer than 20-mers (entanglement length for the homopolymers is close to 32[6] in this model). But in order to minimize the finite size effects, the simulation box length must be several times longer than the length of the homopolymers as suggested by Won Ho Jo *et al.*[39] Since polymer blends are dense ($\phi = 0.5$ for our system) we find that for box lengths above 80 ($L > 80$), the simulations become computationally demanding. Therefore a box length of 80 ($L = 80$) is chosen as a compromise. We choose to work with 20-mers homopolymers as the box length ($L = 80$) is four times the length of homopolymers; even at the end of the simulation the size of the phase separated domains did not reach the system size for any of the blend systems under consideration. Based on our previous work[22] we find that in order to generate the PLC sequences *via* Khokhlov's instantaneous coloring procedure[24,25] the chain length of the parent homopolymer must be at least 30 so that the parent homopolymer can fold back onto itself to form a globule on which the coloring procedure can be performed. Moreover it is easier to ascertain the differences in the compatibilization effectiveness of various copolymer sequences for long copolymer chains. For this reason we choose 70-mers copolymers as they are long enough but at the same time are shorter than the simulation box ($L = 80$) in order to minimize the finite size effects.

In order to characterize statistically the different types of AB copolymer sequences used as compatibilizers we introduce the uniformity factor developed originally by Dadmun.[11] The uniformity factor for component A is defined as:

$$U_A = \left(\left[\sum_{n=1}^{N_C-1} s_n \right] + 1 \right) / \left(N_{typeA} - 1 \right) \quad (1)$$

where s_n is 1 if the n-th and $(n + 1)$-st sphere are type A, −1 if the n-th sphere is type A and the $(n + 1)$-st sphere is type B and 0 if the n-th sphere is B type regardless of the type of $(n + 1)$-st sphere. Here N_C is the total number of monomers in the copolymer and $N_{type\ A}$ is the total number of A monomer segments in the AB copolymer. By definition, compositionally symmetric (*i.e.*, 50% A, 50% B) alternating copolymers possess uniformity factor −1, symmetric diblock copolymers have uniformity factor 1, and random copolymers have uniformity factor 0. The uniformity factor for symmetric PLCs and simple linear gradient copolymers should lie roughly halfway between those for random and diblock copolymers.

The symmetric random A–B copolymer was generated using the following algorithm. Starting with a homopolymer A, segments were picked randomly and changed to type B if the segment chosen was of type A. This process was repeated till the desired composition was achieved and the uniformity factor for components A and B in the random AB copolymer sequence was reduced to zero.

The simple linear gradient A–B copolymer was generated using the multiblock model proposed recently by Jiang *et al.*[21] Using this approach the gradient copolymer chain of length N_C is segmented into Y intervals of equal lengths $\Delta l = N_C/Y$. Each interval is viewed as a mini A–B diblock sequence, whose composition is specified *via* the local gradient distribution function $g(l)$. The j^{th} interval ($j = 0, 1, 2, \ldots, Y - 1$) begins with an A block in the range $[j\Delta l, (j + F_j)\Delta l]$, followed by a B block in the range $[(j + F_j)\Delta l, (j + 1)\Delta l]$, where F_j is the fraction of A blocks in the j^{th} interval. For a specified $g(l)$, F_j is defined by the following equation:

$$F_j = Y \int_{j/Y}^{(j+1)/Y} g(l)dl \quad (2)$$

where the local gradient distribution function $g(l)$ for a simple linear gradient copolymer is defined by the following equation:

$$g(l) = 1 - l/N_C \quad (3)$$

We chose the linear concentration profile over the non-linear hyperbolic tangent concentration profile for gradient copolymers as it would lead to a more fair comparison amongst the various copolymer sequences considered as compatibilizers. The "tanh-gradient" copolymer with non-linear hyperbolic tangent local concentration profile is described by the following equation:

$$g(l) = \frac{1}{2}\left[1 - \tanh\left\{ \lambda \left(\frac{l}{N_C} - \frac{1}{2} \right) \right\} \right] \quad (4)$$

where λ is a parameter. In the above equation when $\lambda \rightarrow \infty$ we recover the concentration profile of a diblock copolymer while for $\lambda \rightarrow 0$ the concentration profile corresponds to that of

a random copolymer. There is no value of λ at which the "tanh-gradient" copolymer concentration profile reduces to that of the simple linear gradient copolymer. For large values of, λ the "tanh-gradient" copolymer is blockier than PLCs; as a result it is likely that such copolymers would outperform PLCs as compatibilizers. However, the tendency to microphase separate also increases with increasing λ.[16,21] In contrast, for $\lambda \rightarrow 0$ the "tanh-gradient" gradient copolymer is less blocky than PLCs and is likely to underperform PLCs as a compatibilizer. This is why we chose to work with simple linear gradient copolymers.

The symmetric AB PLCs were generated *via* a simulation-based instantaneous coloring procedure originally proposed by Khokhlov *et al.*[24–26] A detailed description of our implementation of Khokhlov's coloring procedure to generate 70-mer AB PLCs *via* discontinuous molecular dynamics (DMD) simulation can be found in our previous work.[22] To prepare the symmetric AB 70-mer PLC, a 70-mer A chain with square well interactions between non-adjacent A monomer segments was initialized in a random coil configuration. Fig. 1a shows a snapshot of a sample initial configuration. DMD simulations were performed on the A chain at a low reduced temperature till the A macromolecule collapsed to a globular conformation as shown in Fig. 1b. The segments in the final globular conformation were sorted in order of their distance from the center of the globule. The 35 segments of type A farthest from the center were colored to be B as depicted in Fig. 1c. The coloring procedure resulted in the creation of a 70-mer AB PLC with a composition $x_A = x_B = 0.5$. After the coloring procedure, the conformation of the AB PLC was relaxed. Fig. 1d displays a snapshot of a symmetric AB 70-mer PLC generated *via* the instantaneous coloring procedure. Fig. 2 illustrates the five copolymer sequences considered (a) diblock, (b) PLC (one sequence realization), (c) simple linear gradient, (d) random (one sequence realization), and (e) alternating.

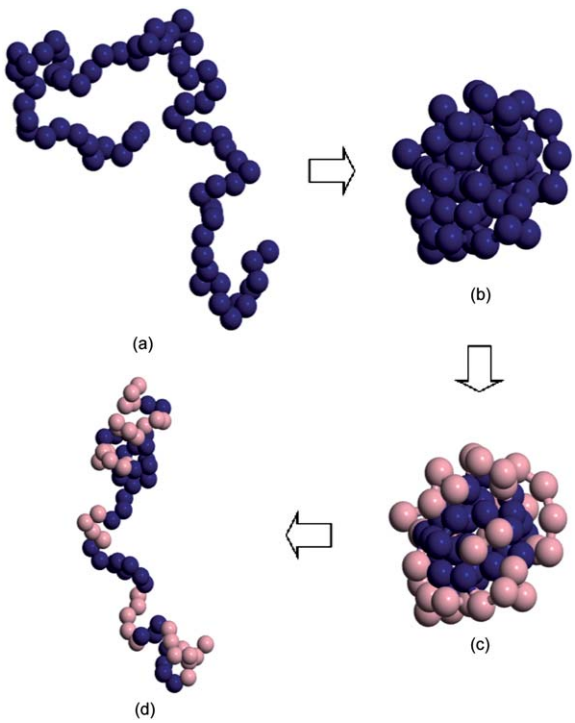

Fig. 1 Snapshots illustrating instantaneous coloring procedure to generate 70-mer A–B PLC (A = dark blue, B = light pink) with composition $x_A = x_B = 0.5$: (a) random configuration of 70-mer A chain, (b) collapsed globular configuration of the A chain, (c) 35 spheres farthest from the center of the globule are colored to type B, and (d) relaxed chain configuration of the resulting A–B 70-mer PLC.

MC simulations are performed on the binary (A/B) and ternary (A/B/A′–B′) blend systems. The simulations on the blend systems are started in a random configuration at the desired volume fraction for all components. Initially the blend systems are mixed uniformly; once the interactions are switched on and MC simulations have been performed for 100,000 Monte Carlo steps (MCS), the systems demix sufficiently into homopolymer A-rich and homopolymer B-rich phases. In each MCS, all segments in the system are moved once on average.

The dynamics of phase separation is monitored by evaluating: 1) the normalized number of nearest-neighbor contacts between segments A–A ($\langle n_{AA}(t)\rangle/\langle n_{AA}(0)\rangle$), B–B ($\langle n_{BB}(t)\rangle/\langle n_{BB}(0)\rangle$), and A–B ($\langle n_{AB}(t)\rangle/\langle n_{AB}(0)\rangle$) where $t = 0$ refers to the initial homogenous state and t refers to time elapsed after the phase separation commences, 2) the fraction of contacts made by the copolymer segments, A′ and B′, with the two different homopolymer segments A and B, $f_{A'A}(t)$, $f_{A'B}(t)$, $f_{B'A}(t)$, and $f_{B'B}(t)$, 3) the copolymer chain expansion ratio, *i.e.*, the normalized copolymer radius of gyration $\langle R_g^2(t)\rangle/\langle R_g^2(0)\rangle$, 4) the spherically-averaged time-dependent collective structure factor $S(q, t)$ for the binary blend and for the ternary compatibilized blends, and 5) the conformation of the copolymers at the interface at the end of the simulation.

The fraction of contacts made by the copolymer segment A′ with the homopolymer segment A is defined to be:

$$f_{A'A}(t) = \langle n_{A'A}(t)/(n_{A'A}(t) + n_{A'B}(t))\rangle \quad (5)$$

where A′ and B′ refer to the A and B segments of the AB copolymer, respectively, and $n_{A'A}(t)$, and $n_{A'B}(t)$ denote the nearest-neighbor contacts between segments A′–A and A′–B, respectively, at time t. Similarly $f_{A'B}(t)$, $f_{B'A}(t)$, and $f_{B'B}(t)$ can also be defined.

The copolymer chain expansion ratio, $\langle R_g^2(t)\rangle/\langle R_g^2(0)\rangle$ is calculated, where $\langle R_g^2(t)\rangle$ is defined by the following equation:

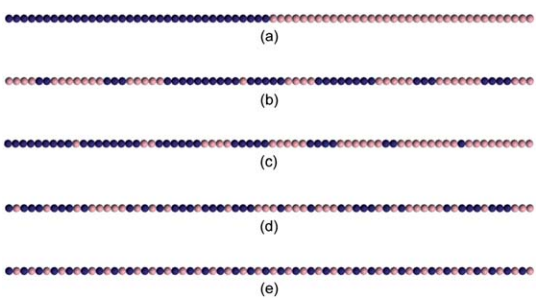

Fig. 2 Sequences of 70-mer A–B copolymers (A = dark blue, B = light pink) with composition $x_A = x_B = 0.5$: (a) diblock, (b) PLC (one sequence realization), (c) simple linear gradient, (d) random (one sequence realization), and (e) alternating.

$$\left\langle R_g^2(t)\right\rangle = \sum_{i=1}^{N_{copolymer}} \sum_{j=1}^{N_C} \left\{r_{i,j}(t) - r_i^{cm}(t)\right\}^2 / \left\{N_{copolymer} N_C\right\} \quad (6)$$

with $\langle R_g^2(t)\rangle$ equal to the copolymer radius of gyration at time t. Here $r_{i,j}(t)$ is the position of the j-th monomer on the i-th copolymer chain at time t and $r_i^{cm}(t)$ is the position of the center of mass of the i-th copolymer chain at time t, $N_{copolymer}$ is the number of copolymer chains.

The time-dependent collective structure factor for both the binary and ternary blend systems[40] is calculated to follow the time evolution of the long-range ordering. The structure factor represents the Fourier transform of the pair correlation function and is defined by the following equation:

$$\boldsymbol{S}(\boldsymbol{q},t) = \left\langle \left[\sum_{r_j} \left(\exp(i\boldsymbol{q}\cdot r_j)\right)(\phi_B^j(t) - \phi_A^j(t) - \left\langle \phi_B^j - \phi_A^j \right\rangle)\right]^2 \right\rangle / L^3 \quad (7)$$

where the scattering vector $\boldsymbol{q}$ is given by $\boldsymbol{q} = 2\pi\boldsymbol{n}/L$ with $\boldsymbol{n}$ equal to a positive integer vector, *i.e.*, $\boldsymbol{n} = (n_x, n_y, n_z)$, the local concentration variable $\phi_A^j(t)$ (or $\phi_B^j(t)$) at time t is equal to one if lattice site j is occupied by an A (or B) segment and zero otherwise. The outer angular bracket $\langle\ldots\rangle$ denotes a thermal statistical average. The contribution from the copolymer chains to the collective structure factor is neglected since we are interested principally in the phase separation of homopolymers A and B, and the copolymer compatibilizer loading ($\approx$4.92%) is small relative to the homopolymers. To improve the statistics in $\boldsymbol{q}$-space the collective structure factor is averaged spherically as follows:

$$S(q,t) = \sum_{q-\left(\frac{\Delta q}{2}\right) \le q \le q+\left(\frac{\Delta q}{2}\right)} \boldsymbol{S}(\boldsymbol{q},t)/m(q,\Delta q) \quad (8)$$

where

$$m(q,\Delta q) = \sum_{q-\left(\frac{\Delta q}{2}\right) \le q \le q+\left(\frac{\Delta q}{2}\right)} 1 \quad (9)$$

denotes the number of lattice points in a spherical shell of radius q with Δq as the shell thickness. In scattering experiments on real immiscible polymer blends, the intensity of scattered radiation, which is related to the structure factor $S(q, t)$ is small initially (for all values of the scattering vector or scattering angle q) as the homopolymers are mixed uniformly. As the phase separation progresses, a distinct peak in the structure factor $S(q^*, t)$ develops at a scattering vector q^*. Physically, at time t, $1/q^*$ represents a measure of the characteristic length scale in the blend while $S(q^*, t)$ is proportional to the difference in concentrations of the constituent homopolymers in the polymer blend.

We also determine the conformation of the copolymers at the interface at the end of the simulation. To do so we move along a copolymer chain and for a given copolymer segment we calculate the difference between the number of nearest-neighbor contacts of that copolymer segment with homopolymer segment A and with homopolymer segment B, $\langle N_A - N_B\rangle$. If $\langle N_A - N_B\rangle$ is large and positive it implies that the copolymer segment resides preferentially in the homopolymer A-rich phase, while a small and negative value of $\langle N_A - N_B\rangle$ signifies that the copolymer segment lies preferentially in the homopolymer B-rich phase.

The system properties for both the binary and ternary blends were averaged over five simulation runs starting from uncorrelated random initial configurations. The results for ternary blends compatibilized by PLCs or random copolymers were averaged over five different copolymer sequences for a given initial configuration. Thus, 50 simulations were performed for ternary blends compatibilized by either PLCs or random copolymers. The errors which represent the sample standard deviations of the properties calculated were within 5%. We chose not to display the errors bars, which are relatively small, on the plots for the sake of clarity.

Results and discussion

Snapshots of the asymmetric binary blend system at various times during the demixing process are presented in Fig. 3. Specifically, Fig. 3 shows the binary blend (**a**) initially, (**b**) at a very early stage in the simulation (5k MCS), (**c**) halfway through the simulation (50k MCS), and (**d**) at the end of the simulation (100k MCS). As the phase separation progresses, homopolymer A-rich and homopolymer B-rich domains begin to form and grow. Fig. 4 shows the ternary A/B/A′–B′ blend compatibilized with the PLC (**a**) initially, (**b**) at a very early stage in the simulation (5k MCS), (**c**) halfway through the simulation (50k MCS), and (**d**) at the end of the simulation (100k MCS). Comparison of Fig. 3 and 4 provides a simple visual comparison of how the presence of the PLC compatibilizer retards the phase separation of the A/B binary blend. In the PLC-compatibilized ternary blend, homopolymer A-rich and homopolymer B-rich

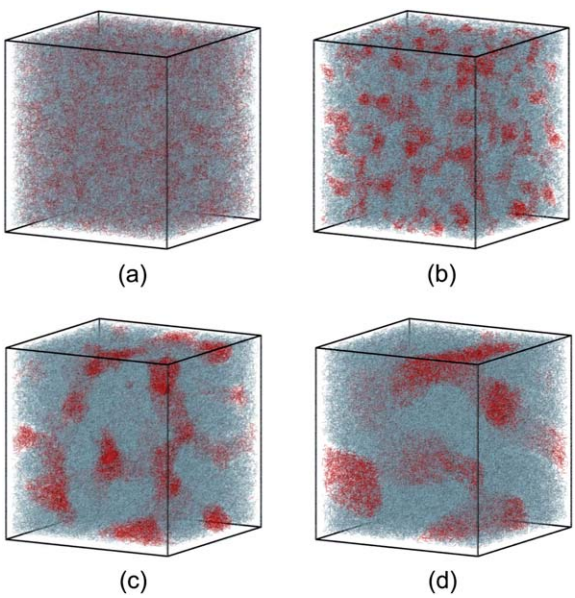

Fig. 3 Simulation snapshots of the A/B binary blend (A = light blue, B = red) at time: (a) $t = 0$ (initial configuration), (b) t = 5k MCS (early stage configuration), (c) t = 50k MCS (halfway configuration), and (d) t = 100k MCS (final configuration).

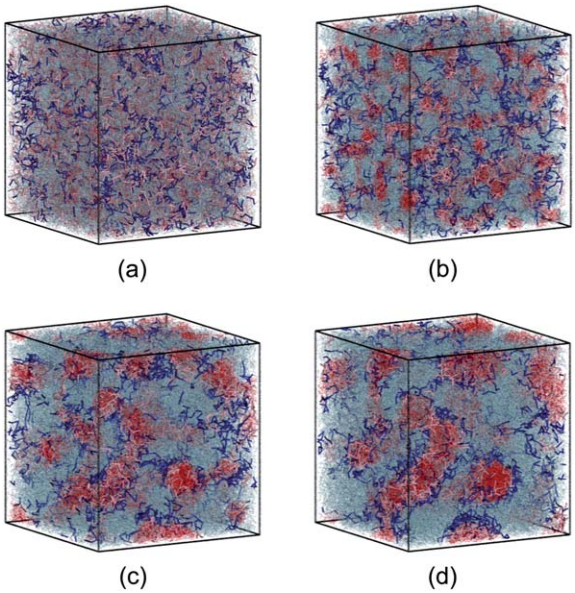

Fig. 4 Simulation snapshots of the PLC compatibilized A/B/A′–B′ blend (A = light blue, B = red, A′ = dark blue, B′ = light pink) at time: (a) t = 0 (initial configuration), (b) t = 5k MCS (early stage configuration), (c) t = 50k MCS (intermediate configuration), and (d) t = 100k MCS (final configuration).

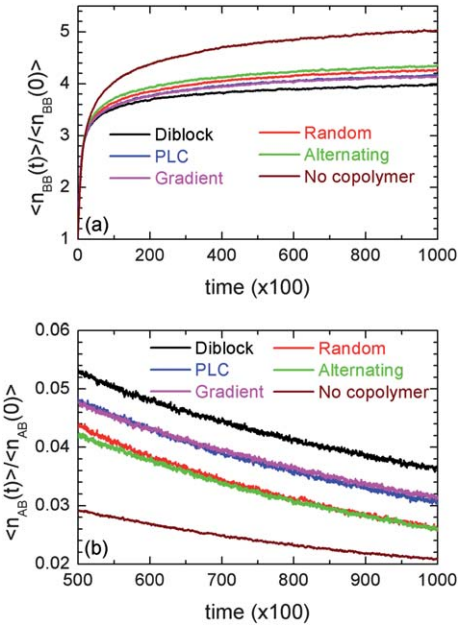

Fig. 5 Normalized contacts for copolymer compatibilized blends with phase separation time: (a) B–B contacts $\langle n_{BB}(t)\rangle/\langle n_{BB}(0)\rangle$ and (b) A–B contacts $\langle n_{AA}(t)\rangle/\langle n_{AA}(0)\rangle$.

domains form and grow as was the case for the pure binary blend; this time, however, the PLCs migrate to the A/B biphasic interface, reducing unfavorable contacts, minimizing interfacial energy and binding the two homopolymer phases together. Similar behavior is observed for the ternary blends compatibilized by diblock, simple linear gradient, random, and alternating copolymers.

The evolving morphology of the binary blend (no copolymer) and ternary compatibilized blends with increasing phase separation are similar in the sense that homopolymer B rich domains (minor phase) form and grow in the matrix of homopolymer A (major phase); this is where the similarity ends and the size of the dispersed domains depends on the blend system and the sequence of the copolymer compatibilizer. Based on the simulation snapshots presented for the various blend systems (*cf.* Fig. 3, Fig. 4, and Fig. 9) the morphologies are different for the various blend systems even after infinite time when thermodynamic equilibrium is achieved. It will soon be evident from the results presented below that at any instant of time during the phase separation (including infinitely long times) the size of the phase separated domains for the binary blends will be a lot larger (or the dispersed domains are more coarse for the binary blend) than for any of the ternary compatibilized blends. The ternary blends compatibilized by diblocks possess the smallest dispersed domains followed by those of PLCs and gradient (which are similar), random, and alternating copolymers.

The process of phase separation in both binary and ternary blends is accompanied by a change in the number of A–A, B–B, and A–B contacts with time. We expect the number of A–A, and B–B contacts to increase and the number of A–B contacts to decrease with increasing phase separation time. In Fig. 5a we plot the normalized number of B–B contacts $\langle n_{BB}(t)/n_{BB}(0)\rangle$ *versus* time. The $\langle n_{BB}(t)/n_{BB}(0)\rangle$ is lowest for diblock copolymers followed by those for PLCs and simple linear gradient copolymers (which are similar), random, and alternating copolymers. The $\langle n_{BB}(t)/n_{BB}(0)\rangle$ for all the ternary blends compatibilized by various copolymer sequences is lower than those for the binary (*i.e.*, no-copolymer) blend, indicating that all copolymers act effectively as compatibilizers. In Fig. 5b we plot the normalized number of A–B contacts $\langle n_{AB}(t)/n_{AB}(0)\rangle$ *versus* time, where, for clarity, time is restricted to the latter half of the simulation. The $\langle n_{AB}(t)/n_{AB}(0)\rangle$ is highest for diblock copolymers followed by those for PLCs and simple linear gradient copolymers (which are similar), random, and alternating copolymers. The $\langle n_{AB}(t)/n_{AB}(0)\rangle$ for all the ternary blends compatibilized by various copolymer sequences is higher than those for the binary (*i.e.*, no-copolymer) blend. Note that the higher the value of $\langle n_{AB}(t)/n_{AB}(0)\rangle$ or the lower the value of $\langle n_{BB}(t)/n_{BB}(0)\rangle$ the greater the extent of mixing between the two immiscible homopolymers. Copolymers, which maximize $\langle n_{AB}(t)/n_{AB}(0)\rangle$ or minimize $\langle n_{BB}(t)/n_{BB}(0)\rangle$, are effective compatibilizers and hence, based on this criteria, diblocks are the best compatibilizers followed by PLCs and gradient (which are similar), random, and alternating copolymers.

As the phase separation evolves in ternary compatibilized blends, the copolymers migrate to the biphasic interface between the two homopolymers and penetrate the homopolymer-rich phases. To monitor the extent of penetration of copolymers into the homopolymer-rich phases, we record the fraction of contacts made by the copolymer segment A′ with the homopolymer segment A $f_{A'A}(t)$ and similarly, $f_{A'B}(t)$, $f_{B'A}(t)$, and $f_{B'B}(t)$. In Fig. 6a we plot $f_{A'A}(t)$ *versus* phase separation time. The $f_{A'A}(t)$ increases with time, as expected, for diblock, PLC and simple linear gradient copolymers since the interaction between components A′ (A′ refers to the component A on the AB

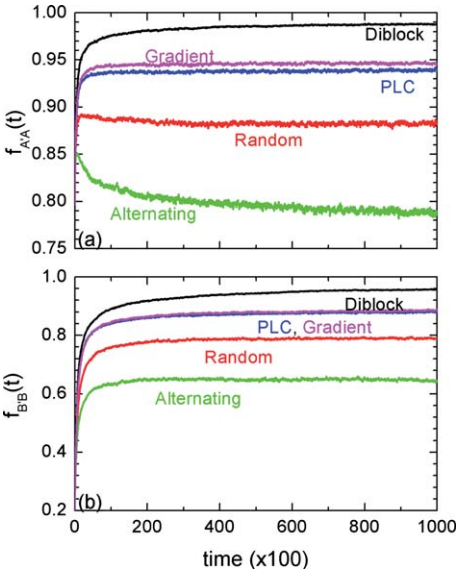

Fig. 6 Fraction of the nearest-neighbor contacts between the copolymer and homopolymer segments with phase separation in ternary compatibilized blends: (a) $f_{A'A}(t)$ and (b) $f_{B'B}(t)$.

copolymer) and A is favorable. However, $f_{A'A}(t)$ decreases with time for alternating and random copolymers. The increase in $f_{B'B}(t)$ with increasing time for all copolymer sequences as shown in Fig. 6b. A plausible reason for this counterintuitive behavior for random and alternating copolymers is that they are pushed preferentially into the homopolymer B-rich phase (minor phase) at the biphasic interface. The $f_{A'A}(t)$ and $f_{B'B}(t)$ are highest for diblock copolymers followed by those for PLCs and simple linear gradient copolymers (which are similar), random, and alternating copolymers; concordantly, diblocks are the best compatibilizers followed by PLCs and gradient (which are similar), random, and alternating copolymers.

Fig. 7 displays the copolymer chain expansion ratio, or normalized radius of gyration $\langle R_g^2(t)\rangle/\langle R_g^2(0)\rangle$, as a function of time. The ratio $\langle R_g^2(t)\rangle/\langle R_g^2(0)\rangle$ increases for all copolymer sequences with increasing time as expected except for alternating copolymers. An effective copolymer compatibilizer is likely to exhibit a relatively high chain expansion since this would signify greater stretching and the increased likelihood of copolymer

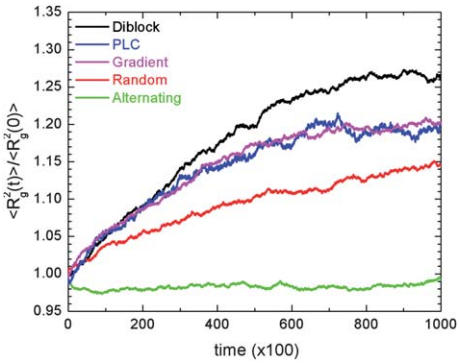

Fig. 7 Copolymer normalized radius of gyration $\langle R_g^2(t)\rangle/\langle R_g^2(0)\rangle$ with phase separation time for ternary compatibilized blends.

penetration into the homopolymer-rich phases. Diblock copolymers stretch most as they have the highest $\langle R_g^2(t)\rangle/\langle R_g^2(0)\rangle$ followed by PLCs and simple linear gradient copolymers (which are similar), random, and alternating copolymers. The ratio $\langle R_g^2(t)\rangle/\langle R_g^2(0)\rangle$ for alternating copolymers does not change significantly with time unlike any other copolymer sequences considered; alternating copolymers end up lying along the interface (*cf.* Fig. 9e and Fig. 10) at the end of the simulation. The overall radius of gyration $\langle R_g^2(t)\rangle$ of the copolymer offers insight into the dimension of the copolymer but not into its orientation with respect to the interface. To gain further insight into the orientation of the copolymer at the interface it is vital to calculate the radii of gyration parallel (or along) $\langle R_g^2(t)\rangle_{\|}$ and perpendicular (or normal) $\langle R_g^2(t)\rangle_{\perp}$ to the interface. For the current study it is challenging to compute $\langle R_g^2(t)\rangle_{\|}$ and $\langle R_g^2(t)\rangle_{\perp}$ as the interface is curved and keeps on changing with time as the demixing occurs. In our recent previous computer simulations studies of the equilibrium properties of PLCs, diblock, random, and alternating copolymer compatibilizers[22] we were able to compute $\langle R_g^2(t)\rangle_{\|}$ and $\langle R_g^2(t)\rangle_{\perp}$ for the various copolymer sequences at low reduced temperatures easily as a nearly flat biphasic interface formed between the two immiscible homopolymers. We found that for a given reduced temperature $\langle R_g^2\rangle_{\|} > \langle R_g^2\rangle_{\perp}$ for alternating copolymers as they lie at the biphasic interface. Therefore it is quite possible that $\langle R_g^2(t)\rangle_{\|}$ increases with time but $\langle R_g^2(t)\rangle_{\perp}$

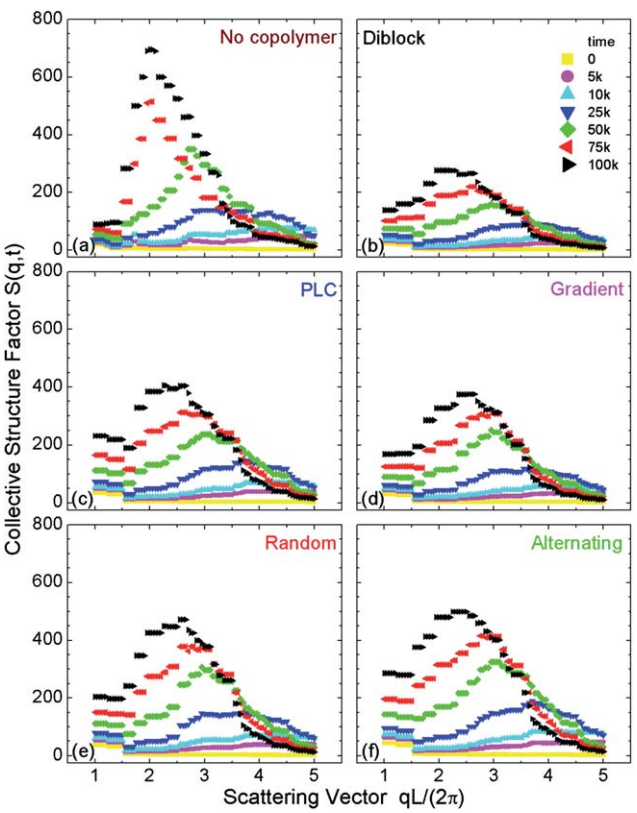

Fig. 8 Evolution of $S(q, t)$ with phase separation time for: (a) binary blend (no copolymer), (b) diblock copolymer ternary blend, (c) PLC ternary blend, (d) gradient copolymer ternary blend, (e) random copolymer ternary blend, and (f) alternating copolymer ternary blend.

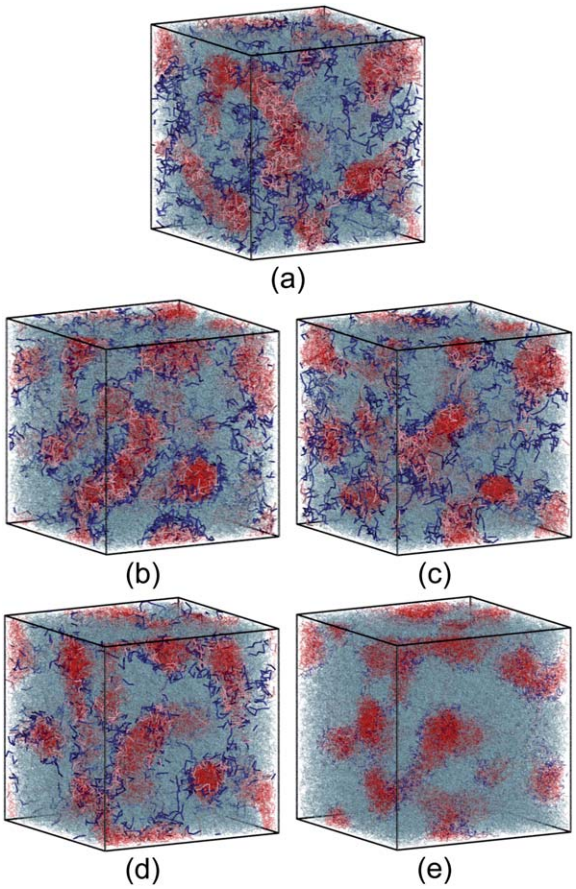

Fig. 9 Simulation snapshots of the binary blend compatibilized by various copolymer sequences at the end of the simulation: (a) diblock, (b) PLC, (c) simple linear gradient, (d) random, and (e) alternating.

decreases with time for alternating copolymers and $\langle R_g^2(t)\rangle$ does not change significantly with time.

To quantify the extent of phase separation in both the binary and ternary compatibilized blends, we determine the spherically-averaged time-dependent collective structure factor $S(q, t)$. Fig. 8 shows a plot of $S(q, t)$ as a function of the scattering vector for both the binary and ternary (*i.e.*, compatibilized) blends. Initially $S(q, t)$ is small for all cases as the blend is homogeneous. With increasing phase separation time a distinct peak develops and the location of the peak shifts towards smaller values of the scattering vector, signifying the growth in size of the phase-separated domains. This behavior is also observed in light scattering experiments on real polymer blends.[41–51] An efficient compatibilizer would suppress the height of the peak in $S(q, t)$ and shift it to higher values of the scattering vector. The structure factor for the binary blend without any copolymer compatibilizer is shown in Fig. 8a. The $S(q, t)$ for the diblock, PLC, simple linear gradient, random, and alternating copolymer compatibilized blends are shown in Fig. 8b through 8f, respectively. Based on the $S(q, t)$ calculations, diblock copolymers are most effective in slowing down the process of phase separation because they have the smallest $S(q, t)$, followed by PLCs and simple linear gradient copolymers (which are similar), random, and alternating copolymers. All copolymers irrespective of their sequence slow down the phase separation in compatibilized blends in comparison to the binary blend (no-copolymer).

Fig. 9 depicts the simulation snapshots for each of the five compatibilized blends with ≈4.92% copolymer at the end of the simulation. Each block of the diblock copolymer (Fig. 9a) penetrates the homopolymer-rich phases on either side of the interface. Alternating copolymers (Fig. 9e) prefer to lie at the interface. Random copolymers (Fig. 9b), PLCs (Fig. 9d), and simple linear gradient copolymers (Fig. 9c) weave back and forth across the biphasic interface binding the two homopolymer rich phases together.

To establish the conformation of the copolymers at the interface and the mechanism by which they stabilize the interface, we calculate the difference between the number of nearest-neighbor contacts of that copolymer segment with homopolymer segment A, and with homopolymer segment B, $\langle N_A - N_B\rangle$ for each copolymer segment along the copolymer chain at the end of the simulation. Fig. 10 depicts $\langle N_A - N_B\rangle$ along the copolymer chain for various copolymer sequences. A large and positive value of $\langle N_A - N_B\rangle$ for a particular copolymer segment indicates that the copolymer segment lies in the homopolymer A-rich phase. A small and negative value of $\langle N_A - N_B\rangle$ for a particular copolymer segment indicates that the copolymer segment lies in the homopolymer B-rich phase. From the data in Fig. 10 it is evident that each block of the diblock copolymer penetrates the energetically favorable homopolymer-rich phase *i.e.*, A′ penetrates A and B′ penetrates B. Alternating copolymers lie at the interface as the value of $\langle N_A - N_B\rangle$ is close to zero. PLCs, simple linear gradient and random copolymers weave back and forth across the interface. The weaving and penetration across the interface is pronounced for PLCs in comparison to random copolymers, while that of gradient copolymers are on a par with the behavior seen in PLCs. This analysis is useful because we do not have to make any *a priori* assumptions about the flatness of the biphasic interface between the two homopolymers.

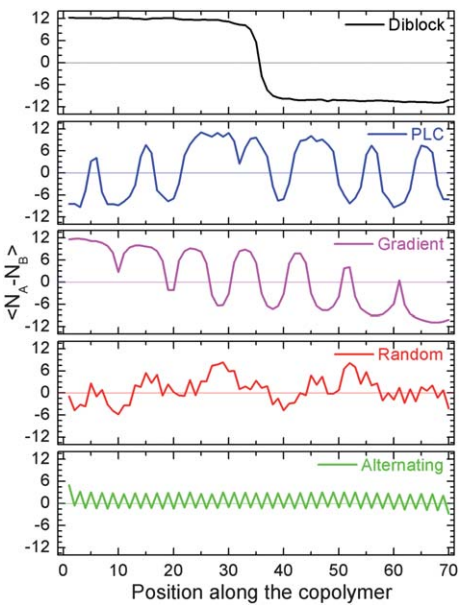

Fig. 10 Orientation of the copolymers at the interface at the end of the simulation.

It is of interest to compare our results with the lattice MC simulations of Ko *et al.*,[7] who reported that diblock copolymers were the best compatibilizers followed by random-block, random, random-alternating, and alternating copolymers. The relative compatibilization performance of diblock, random, and alternating copolymers as suggested by our simulations are in good agreement with the results of Ko *et al.*[7] The simulation results from Ko *et al.*'s work on random-block (uniformity factor of 0.5) copolymers cannot be equated with those of PLCs for comparison purposes because random-block copolymers have a sequence distribution that is different from that of PLCs. Khokhlov and coworkers[52] have demonstrated that random-block copolymers (whose block length obeys a Poisson distribution) are statistically different from PLCs (which obey Levy flight statistics for the block length), despite having the same composition and average block length (or uniformity factor) for both types of copolymers. Our results on the performance of PLCs as compatibilizers relative to those of diblock, random, and alternating copolymers are consistent with our previous work involving DMD simulations.[22]

As mentioned several times earlier, the compatibilizing performance of simple linear gradient copolymers, which have a highly ordered sequence, is on a par with that of PLCs. One plausible reason for this is that the degree of blockiness of PLCs is comparable to that of simple linear gradient copolymers. Another reason is that unlike PLCs, simple linear gradient A–B copolymers possess long blocks of type A adjacent to short blocks of type B on the one end of the copolymer and *vice versa* on the other end of the copolymer, and the long blocks of type A prefer to penetrate the homopolymer A-rich phase. While doing so, they drag successfully along the short adjacent blocks of type B leading to higher interfacial energy and poor weaving across the biphasic interface.

Although we have presented results only for copolymer concentration of $\approx$4.92%, computer simulations for higher copolymer loadings, *i.e.*, $\approx$19.69%, have also been performed. The trends amongst the various copolymer sequences observed at $\approx$4.92% copolymer concentration also hold true for the higher copolymer concentration $\approx$19.69%. Interestingly the diblock did not microphase separate even at this higher copolymer concentration, most likely because the homopolymers in our simulations are much shorter than the diblock copolymers. Previous studies[53–59] on diblock-copolymer compatibilized ternary polymer blends have shown that for microphase separation of diblock to occur, the diblock concentration must be high ($\approx$20%), the effective interaction strength parameter must be large ($\chi_{AB}L_{copolymer} > 10.5$), and the homopolymers must be much longer than each block of the diblock copolymer. We chose to perform kinetic MC simulations on ternary polymer blends with short (20-mer) homopolymer chains because working with very long homopolymer chains (relative to the copolymers) would require a bigger simulation box to minimize the finite size effects, and this would have been too computationally demanding. It would be interesting to study the compatibilization effectiveness of various copolymer sequences in immiscible binary polymer blends at high copolymer concentrations with very long homopolymers relative to the copolymer as it is likely that the diblock as well as simple linear gradient copolymers might microphase separate easily, unlike PLCs. PLCs might thus be the most effective compatibilizers. We acknowledge that the polymers (20-mers homopolymers and 70-mers copolymers) used in our work might not be representative of industrially relevant high molecular polymers (100-mers or even longer). However, the compatibilization effectiveness trends amongst the various copolymer sequences would still hold even for polymers longer than those studied here. Self-consistent field theory (SCFT) studies of compatibilized blends with higher copolymer concentrations and very long homopolymers relative to the copolymer chain lengths are in progress and will be the subject of future publications.

Conclusions

We presented the results of kinetic Monte Carlo simulations aimed at exploring the effect of co-monomer sequence in copolymer compatibilizers on the dynamics of phase separation of incompatible A/B binary homopolymer blends. Diblock, PLCs, simple linear gradient, random, and alternating copolymers made of equal numbers of A and B segments and identical chain lengths were considered as compatibilizers. In binary blends the process of phase separation was accompanied by the formation and growth of homopolymer B (minor homopolymer phase) rich domains dispersed in a matrix of homopolymer A (major homopolymer phase). In ternary compatibilized blends all copolymers irrespective of their sequence retarded the process of phase separation by migrating to the biphasic interface between the two incompatible homopolymers, thus minimizing the interfacial energy and promoting adhesion.

The normalized number of nearest neighbor contacts between homopolymer segments A and B or between B and B were recorded to monitor the process of phase separation. For all the blend systems the number of A–B contacts decreased with time while the number of the B–B contacts increased with time, indicating the demixing of the blend. Diblock copolymers maximized the normalized number of A–B contacts and minimized the normalized number of B–B contacts, followed by PLCs and simple linear gradient copolymers (which were similar), random, and alternating copolymers. The fraction of PLC contacts with homopolymer segments, A′–A and B′–B, were recorded to monitor the extent of penetration of copolymers into the homopolymer rich phase. The fraction of A′–A contacts increased with time for all sequences except random and alternating copolymers, while the fraction of B′–B contacts increased for all copolymer sequences. A plausible explanation for this counterintuitive behavior for random and alternating copolymers is that they are pushed preferentially into the homopolymer B-rich phase (minor phase) at the biphasic interface. Diblock copolymers maximized the fraction of A′–A, and B′–B contacts followed by PLCs and simple linear gradient copolymers (which were similar), random, and alternating copolymers.

We calculated the time-dependent collective structure factor $S(q, t)$ for all the blend systems to monitor the dynamics of phase separation. Diblock copolymers were most effective in slowing down the process of phase separation as they had the smallest $S(q, t)$, followed by PLCs and simple linear gradient copolymers (which were similar), random, and alternating copolymers. All

copolymers irrespective of their sequence succeeded in slowing down the phase in immiscible binary polymer blends.

Diblock copolymers stretched the most at the interface as deduced from the highest chain expansion ratio followed by PLCs and simple linear gradient copolymers (which were similar), random, and alternating copolymers. The chain expansion ratio increased with time for all copolymer sequences.

We monitored the conformation of the copolymers at the interface by evaluating the difference between the number of nearest-neighbor contacts of that copolymer segment with homopolymer segment A and with homopolymer segment B at the end of the simulation for each copolymer segment along the copolymer chain. No assumption was made about the flatness of the interface. Each block of the diblock copolymer penetrated the homopolymer rich phase on either side of the interface. Alternating copolymers preferred to lie at the interface. Random, PLCs and simple linear gradient copolymers weaved back and forth across the interface, binding the two homopolymer rich phases together. The weaving and penetration was more pronounced for PLCs than for random or simple linear gradient copolymers.

Our results are in good agreement with the lattice Monte Carlo simulations of Ko *et al.*[7] for diblock, random, and alternating copolymers. Our results on the performance of PLCs as compatibilizers relative to those of diblock, random, and alternating copolymers are in excellent agreement with our previous work involving DMD simulations on PLCs.[22] A surprising result of our work is the compatibilizing ability of PLCs observed here in on a par with that of simple linear gradient copolymers, which have received a great deal of attention as potential alternatives to diblock copolymers for use as compatibilizers.[12–21] Compared to diblock and gradient copolymers, which are synthesized *via* controlled free radical polymerization,[14,27–32] PLCs are relatively easy to prepare *via* the coloring reaction described by Genzer and coworkers.[60] PLCs thus have real potential as compatibilizers for immiscible polymer blends. In a nutshell, the copolymer sequence plays a dominant role in determining its ability to effectively act as a compatibilizer for immiscible blends.

Acknowledgements

This work was supported by the Director, Office of Energy Research, Office of Basic Sciences, Chemical Science Division of the U.S. Department of Energy under Grant DE-FG05-91ER14181 awarded to C. K. H. J. G. thanks the National Science Foundation for financial support through Grants No. DMR-0353102 and OISE-0730243.

References

1 L. Leibler, Theory of Microphase Separation in Block Co-Polymers, *Macromolecules*, 1980, **13**, 1602–1617.
2 L. Leibler, Emulsifying Effects of Block Copolymers in Incompatible Polymer Blends, *Makromol. Chem., Macromol. Symp.*, 1988, **16**, 1–17.
3 H. Tanaka and T. Hashimoto, Stability Limits for Macro-Phase and Microphase Transitions and Compatibilizing Effects in Mixtures of A–B Block Polymers with Corresponding Homopolymers, *Polymer Communications*, 1988, **29**, 212–216.
4 K. R. Shull, E. J. Kramer, G. Hadziioannou and W. Tang, Segregation of Block Copolymers to Interfaces between Immiscible Homopolymers, *Macromolecules*, 1990, **23**, 4780–4787.
5 K. R. Shull, K. I. Winey, E. L. Thomas and E. J. Kramer, Segregation of Block Copolymer Micelles to Surfaces and Interfaces, *Macromolecules*, 1991, **24**, 2748–2751.
6 S. Y. Kamath and M. D. Dadmun, The effect of chain architecture on the dynamics of copolymers in a homopolymer matrix: Lattice Monte Carlo simulations using the bond-fluctuation model, *Macromol. Theory Simul.*, 2005, **14**, 519–527, DOI: 10.1002/mats.200500023.
7 M. J. Ko, S. H. Kim and W. H. Jo, The effects of copolymer architecture on phase separation dynamics of immiscible homopolymer blends in the presence of copolymer: a Monte Carlo simulation, *Polymer*, 2000, **41**, 6387–6394.
8 A. C. Balazs and M. T. Demeuse, Miscibility in Ternary Mixtures Containing a Copolymer and 2 Homopolymers - Effect of Sequence Distribution, *Macromolecules*, 1989, **22**, 4260–4267.
9 A. C. Balazs, I. C. Sanchez, I. R. Epstein, F. E. Karasz and W. J. Macknight, Effect of Sequence Distribution on the Miscibility of Polymer Copolymer Blends, *Macromolecules*, 1985, **18**, 2188–2191.
10 Y. Lyatskaya, D. Gersappe, N. A. Gross and A. C. Balazs, Designing compatibilizers to reduce interfacial tension in polymer blends, *J. Phys. Chem.*, 1996, **100**, 1449–1458.
11 M. Dadmun, Effect of copolymer architecture on the interfacial structure and miscibility of a ternary polymer blend containing a copolymer and two homopolymers, *Macromolecules*, 1996, **29**, 3868–3874.
12 J. Kim, M. K. Gray, H. Y. Zhou, S. T. Nguyen and J. M. Torkelson, Polymer blend compatibilization by gradient copolymer addition during melt processing: Stabilization of dispersed phase to static coarsening, *Macromolecules*, 2005, **38**, 1037–1040, DOI: 10.1021/ma047549t.
13 J. Kim, R. W. Sandoval, C. M. Dettmer, S. T. Nguyen and J. M. Torkelson, Compatibilized polymer blends with nanoscale or sub-micron dispersed phases achieved by hydrogen-bonding effects: Block copolymer *vs.* blocky gradient copolymer addition, *Polymer*, 2008, **49**, 2686–2697, DOI: 10.1016/j.polymer.2008.04.008.
14 J. Kim, H. Y. Zhou, S. T. Nguyen and J. M. Torkelson, Synthesis and application of styrene/4-hydroxystyrene gradient copolymers made by controlled radical polymerization: Compatibilization of immiscible polymer blends *via* hydrogen-bonding effects, *Polymer*, 2006, **47**, 5799–5809, DOI: 10.1016/j.polymer.2006.06.030.
15 Y. Tao, J. Kim and J. M. Torkelson, Achievement of quasi-nanostructured polymer blends by solid-state shear pulverization and compatibilization by gradient copolymer addition, *Polymer*, 2006, **47**, 6773–6781, DOI: 10.1016/j.polymer.2006.06.030.
16 R. Wang, *et al.*, Phase Behavior of Ternary Homopolymer/Gradient Copolymer Blends, *Macromolecules*, 2009, **42**, 2275–2285, DOI: 10.1021/ma801398a.
17 K. R. Shull, Interfacial activity of gradient copolymers, *Macromolecules*, 2002, **35**, 8631–8639, DOI: 10.1021/ma020698w.
18 M. D. Lefebvre, *et al.*, Effect of sequence distribution on copolymer interfacial activity, *Macromolecules*, 2005, **38**, 10494–10502, DOI: 10.1021/ma0509762.
19 A. Aksimentiev and R. Holyst, Phase behavior of gradient copolymers, *J. Chem. Phys.*, 1999, **111**, 2329–2339.
20 A. Aksimentiev and R. Holyst, Phase behavior of gradient copolymers, *Aip Conf Proc*, 2000, **519**(71–77), 800.
21 R. Jiang, *et al.*, Phase behavior of gradient copolymers, *Macromolecules*, 2008, **41**, 5457–5465, DOI: 10.1021/ma8002517.
22 R. Malik, C. K. Hall and J. Genzer, Protein-Like Copolymers (PLCs) as Compatibilizers for Homopolymer Blends, *Macromolecules*, 2010, **43**, 5149–5157, DOI: 10.1021/ma100460y.
23 R. Malik, C. K. Hall and J. Genzer, Phase Separation Dynamics for a Polymer Blend Compatibilized by Protein-like Copolymers: a Monte Carlo Simulation, *Macromolecules*, DOI: 10.1021/ma2014832.
24 P. G. Khalatur, V. A. Ivanov, N. P. Shusharina and A. R. Khokhlov, Protein-like copolymers: computer simulation, *Russ. Chem. Bull.*, 1998, **47**, 855–860.
25 A. R. Khokhlov and P. G. Khalatur, Protein-like copolymers: Computer simulation, *Phys. A*, 1998, **249**, 253–261.
26 A. R. Khokhlov and P. G. Khalatur, Conformation-dependent sequence design (engineering) of AB copolymers, *Phys. Rev. Lett.*, 1999, **82**, 3456–3459.
27 J. He, Y. F. Wang, Q. F. Lin, L. G. Chen and X. D. Zhou, Synthesis and Characterization of Functional Gradient Copolymers of 2-Hydroxyethyl Methacrylate and tert-Butyl Acrylate by Atom

Transfer Radical Polymerization, *J. Macromol. Sci., Part A: Pure Appl. Chem.*, 2009, **46**, 405–411, DOI: 10.1080/10601320902728702, Pii 909209145.
28 Y. Zhao, Y. W. Luo, C. H. Ye, B. G. Li and S. P. Zhu, Model-Based Design and Synthesis of Gradient MMA/tBMA Copolymers by Computer-Programmed Semibatch Atom Transfer Radical Copolymerization, *J. Polym. Sci., Part A: Polym. Chem.*, 2009, **47**, 69–79, DOI: 10.1002/pola.23121.
29 K. I. Seno, I. Tsujimoto, S. Kanaoka and S. Aoshima, Synthesis of various stimuli-responsive gradient copolymers by living cationic polymerization and their thermally or solvent induced association behavior, *J. Polym. Sci., Part A: Polym. Chem.*, 2008, **46**, 6444–6454, DOI: 10.1002/pola.22953.
30 S. B. Lee, A. J. Russell and K. Matyjaszewski, ATRP synthesis of amphiphilic random, gradient, and block copolymers of 2-(dimethylamino)ethyl methacrylate and n-butyl methacrylate in aqueous media, *Biomacromolecules*, 2003, **4**, 1386–1393, DOI: 10.1021/bm034126a.
31 K. Matyjaszewski, M. J. Ziegler, S. V. Arehart, D. Greszta and T. Pakula, Gradient copolymers by atom transfer radical copolymerization, *J. Phys. Org. Chem.*, 2000, **13**, 775–786.
32 D. Neugehauer and K. Matyjaszewski, Copolymers with spontaneous gradient structure by atom transfer radical copolymerization of PEO (meth)acrylate macromonomers with TMS-ethyl (meth)acrylates, *Abstr Pap Am Chem S*, 2003, **225**, U619–U619.
33 I. Carmesin and K. Kremer, The Bond Fluctuation Method - A New Effective Algorithm for the Dynamics of Polymers in All Spatial Dimensions, *Macromolecules*, 1988, **21**, 2819–2823.
34 W. Paul, K. Binder, D. W. Heermann and K. Kremer, Crossover Scaling in Semidilute Polymer-Solutions - A Monte-Carlo Test, *J. Phys. II*, 1991, **1**, 37–60.
35 W. Paul, K. Binder, D. W. Heermann and K. Kremer, Dynamics of Polymer-Solutions and Melts - Reptation Predictions and Scaling of Relaxation-Times, *J. Chem. Phys.*, 1991, **95**, 7726–7740.
36 J. Baschnagel, K. Binder and H. P. Wittmann, The Influence of the Cooling Rate on the Glass-Transition and the Glassy State in 3-Dimensional Dense Polymer Melts - a Monte-Carlo Study, *J. Phys.: Condens. Matter*, 1993, **5**, 1597–1618.
37 J. Baschnagel and K. Binder, Structural Aspects of a 3-Dimensional Lattice Model for the Glass-Transition of Polymer Melts - a Monte-Carlo Simulation, *Phys. A*, 1994, **204**, 47–75.
38 K. Binder. in *Monte Carlo and Molecular Dynamics Simulations in Polymer Science* **Vol. 17** (Oxford University Press: New York, 1995).
39 W. H. Jo and S. H. Kim, Monte carlo simulation of the phase separation dynamics of polymer blends in the presence of block copolymers.1. Effect of the interaction energy and chain length of the block copolymers, *Macromolecules*, 1996, **29**, 7204–7211.
40 A. Sariban and K. Binder, Spinodal Decomposition of Polymer Mixtures - a Monte-Carlo Simulation, *Macromolecules*, 1991, **24**, 578–592.
41 T. Hashimoto, M. Itakura and H. Hasegawa, Late Stage Spinodal Decomposition of a Binary Polymer Mixture.1. Critical Test of Dynamic Scaling on Scattering Function, *J. Chem. Phys.*, 1986, **85**, 6118–6128.
42 T. Hashimoto, M. Itakura and N. Shimidzu, Late Stage Spinodal Decomposition of a Binary Polymer Mixture.2. Scaling Analyses on Qm(Tau) and Im(Tau), *J. Chem. Phys.*, 1986, **85**, 6773–6786.
43 T. Hashimoto, M. Takenaka and H. Jinnai, Scattering Studies of Self-Assembling Processes of Polymer Blends in Spinodal Decomposition, *J. Appl. Crystallogr.*, 1991, **24**, 457–466.
44 M. Takenaka and T. Hashimoto, Scattering Studies of Self-Assembling Processes of Polymer Blends in Spinodal Decomposition.2. Temperature-Dependence, *J. Chem. Phys.*, 1992, **96**, 6177–6190.
45 T. Izumitani and T. Hashimoto, Slow Spinodal Decomposition in Binary-Liquid Mixtures of Polymers, *J. Chem. Phys.*, 1985, **83**, 3694–3701.
46 M. Takenaka, T. Izumitani and T. Hasimoto, Slow Spinodal Decomposition in Binary-Liquid Mixtures of Polymers.4. Scaled Structure Factor for Later Stage Unmixing, *J. Chem. Phys.*, 1990, **92**, 4566–4575.
47 F. S. Bates and P. Wiltzius, Spinodal Decomposition of a Symmetric Critical Mixture of Deuterated and Protonated Polymer, *J. Chem. Phys.*, 1989, **91**, 3258–3274.
48 C. C. Han, *et al.*, Static and Kinetic-Studies of Polystyrene Poly (Vinylmethylether) Blends, *Polym. Eng. Sci.*, 1986, **26**, 3–8.
49 G. R. Strobl, Structure Evolution During Spinodal Decomposition of Polymer Blends, *Macromolecules*, 1985, **18**, 558–563.
50 T. Hashimoto, K. Sasaki and H. Kawai, Time-Resolved Light-Scattering Studies on The Kinetics of Phase-Separation and Phase Dissolution of Polymer Blends.2. Phase-Separation of Ternary Mixtures of Polymer-A, Polymer-B, and Solvent, *Macromolecules*, 1984, **17**, 2812–2818.
51 T. Hashimoto, J. Kumaki and H. Kawai, Time-Resolved Light-Scattering-Studies on Kinetics of Phase-Separation and Phase Dissolution of Polymer Blends.1. Kinetics of Phase-Separation of a Binary Mixture of Polystyrene and Polyvinyl Methyl-Ether, *Macromolecules*, 1983, **16**, 641–648.
52 E. N. Govorun, *et al.*, Primary sequences of proteinlike copolymers: Levy-flight-type long-range correlations, *Physical Review E*, 2001, **6404**.
53 T. Inoue, T. Soen, T Hashimot and H. Kawai, Studies on Domain Formation of A-B-Type Block Copolymer from Its Solutions. Ternary Polymer Blend of Styrene-Isoprene Block Copolymer with Polystyrene and Polyisoprene, *Macromolecules*, 1970, **3**, 87.
54 R. E. Cohen and A. R. Ramos, Homogeneous and Heterogeneous Blends of Polybutadiene, Polyisoprene, and Corresponding Diblock Copolymers, *Macromolecules*, 1979, **12**, 131–134.
55 K. J. Jeon and R. J. Roe, Solubilization of a Homopolymer in a Block-Copolymer, *Macromolecules*, 1994, **27**, 2439–2447.
56 A. M. Mayes, T. P. Russell, S. K. Satija and C. F. Majkrzak, Homopolymer Distributions in Ordered Block Copolymers, *Macromolecules*, 1992, **25**, 6523–6531.
57 T. Pan, *et al.*, Macrophase *vs.* Microphase Separation in Copolymer Homopolymer Mixtures, *Macromolecules*, 1993, **26**, 2860–2865.
58 K. R. Shull and K. I. Winey, Homopolymer Distributions in Lamellar Copolymer Homopolymer Blends, *Macromolecules*, 1992, **25**, 2637–2644.
59 K. R. Shull, A. M. Mayes and T. P. Russell, Segment Distributions in Lamellar Diblock Copolymers, *Macromolecules*, 1993, **26**, 3929–3936.
60 J. J. Semler, *et al.*, Facile method of controlling monomer sequence distributions in random copolymers, *Adv. Mater.*, 2007, **19**, 2877.

